Supplementary Material

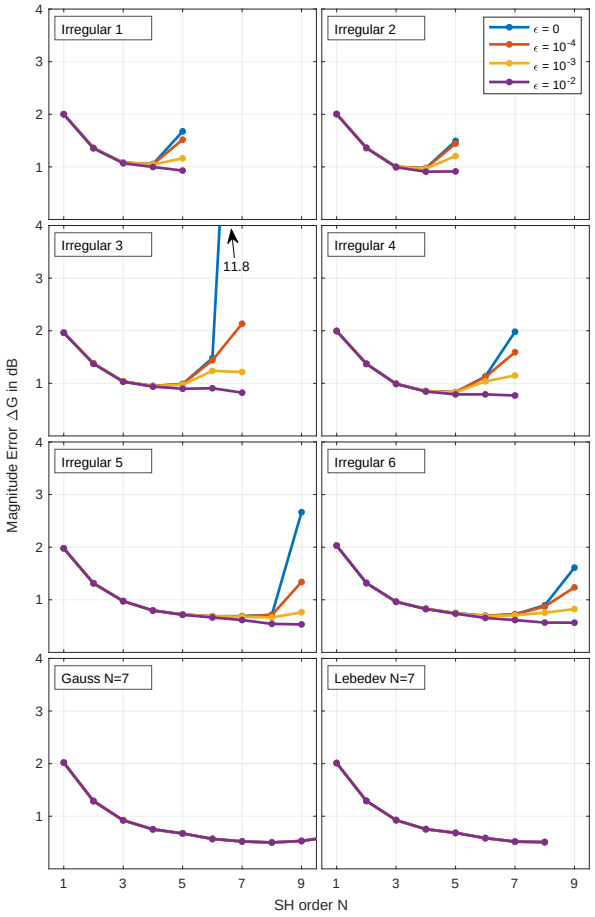

Figure S1. Left-ear magnitude error ΔG with respect to SH order (similar to Figure 2A). Preprocessing of HRTFs prior to SH interpolation: Onset-based time alignment (OBTA) as used by Brinkmann and Weinzierl (2018).

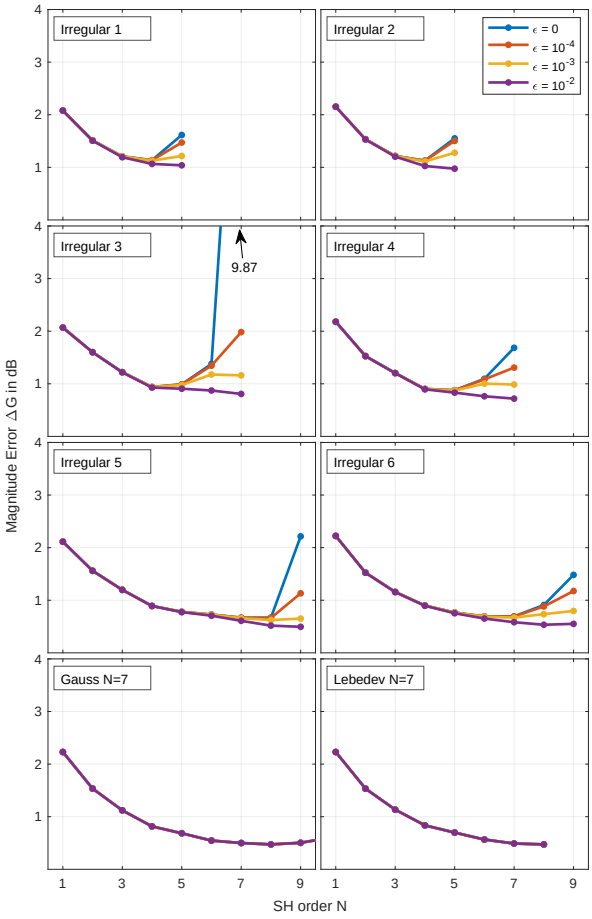

Figure S2. Left-ear magnitude error ΔG with respect to SH order (similar to Figure 2A). Preprocessing of HRTFs prior to SH interpolation: SUpDEq, but only using the phase components of the rigid sphere transfer function.

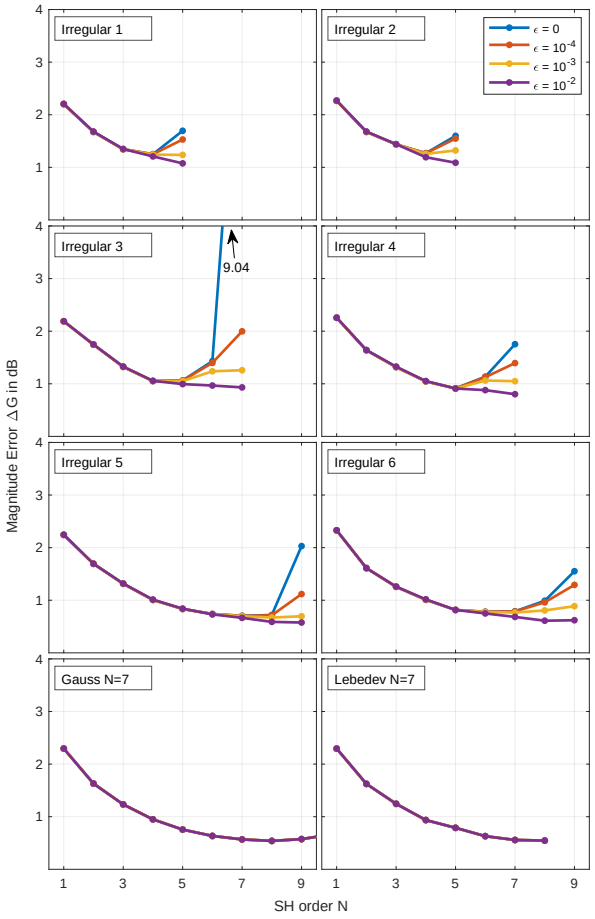

Figure S3. Left-ear magnitude error ΔG with respect to SH order (similar to Figure 2A). Preprocessing of HRTFs prior to SH interpolation: Phase correction as proposed by Ben-Hur et al. (2019).

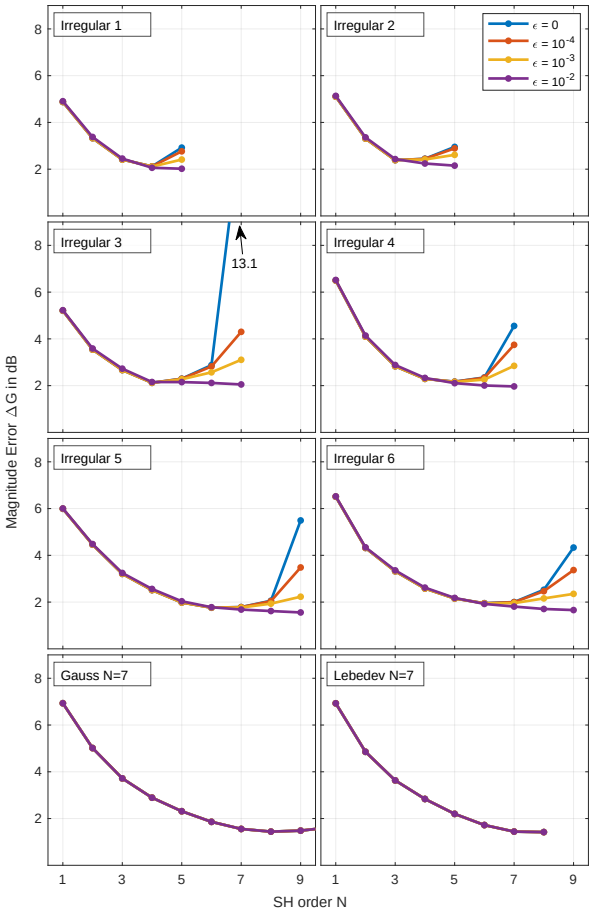

Figure S4. Left-ear magnitude error ΔG with respect to SH order (similar to Figure 2A). No preprocessing applied.

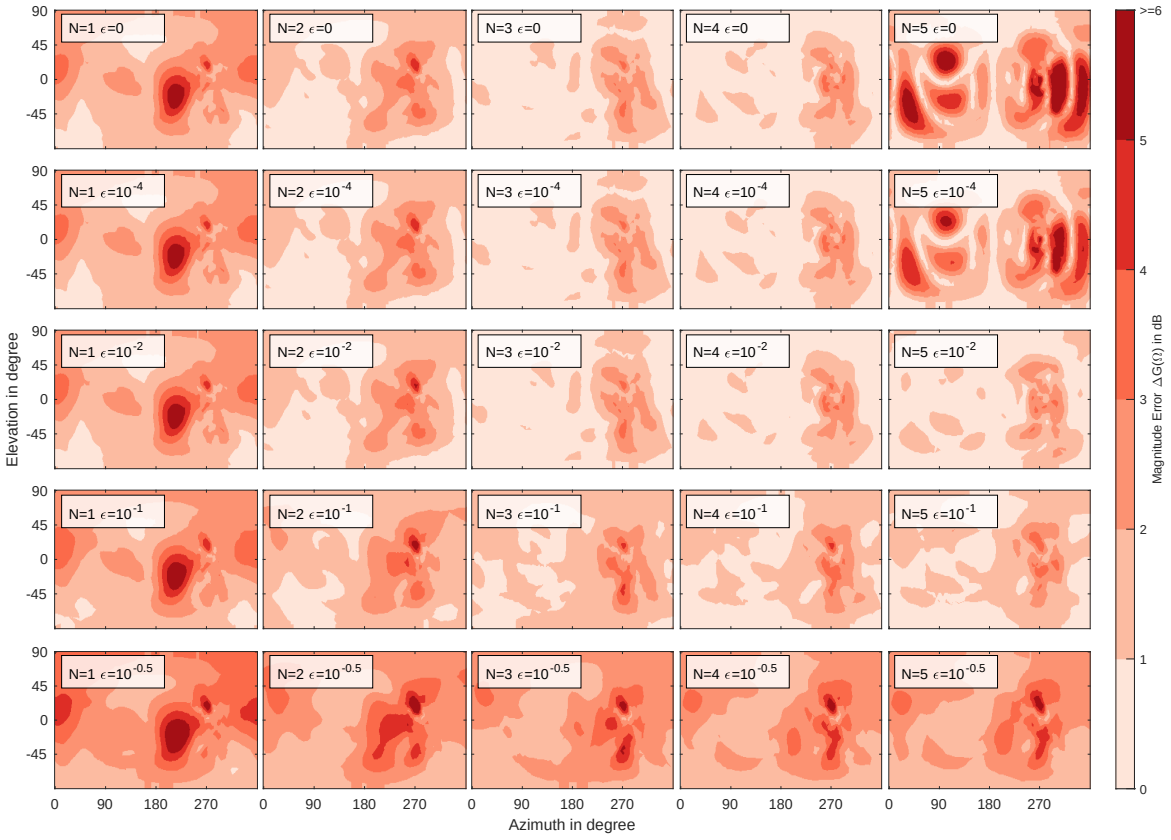

Figure S5. Left-ear magnitude error $\Delta G(\Omega)$ for grid *Irregular 1* at selected SH orders and regularization values ϵ. HRTF: Subject no. 10 from HUTUBS database.

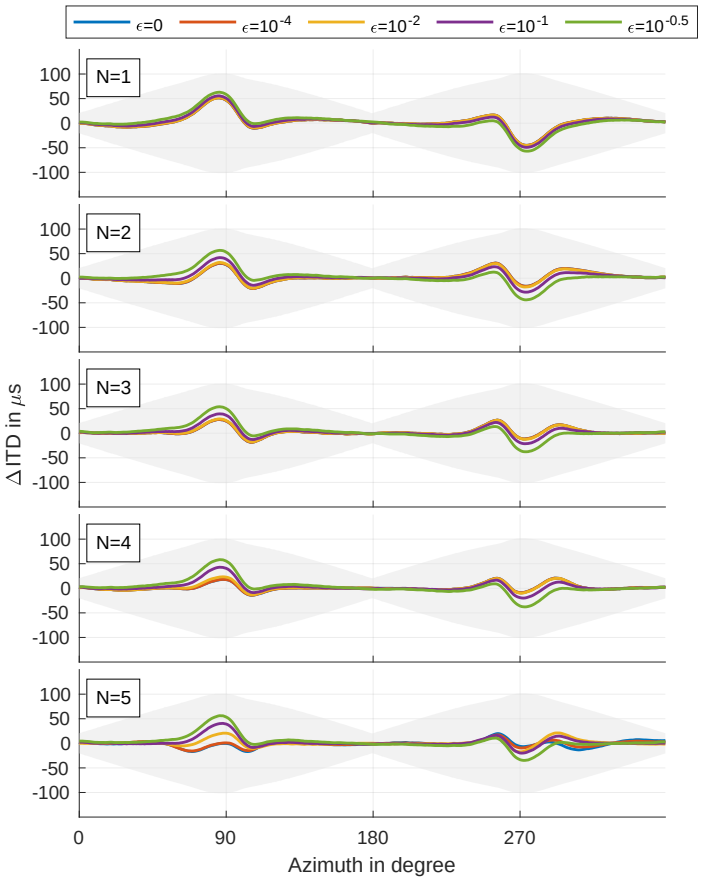

Figure S6. Difference in horizontal plane ITD relative to the dense reference for grid *Irregular 1* at selected SH orders and regularization values ϵ. The shaded area denotes the JND as a function of the reference ITD. HRTF: Subject no. 10 from HUTUBS database.

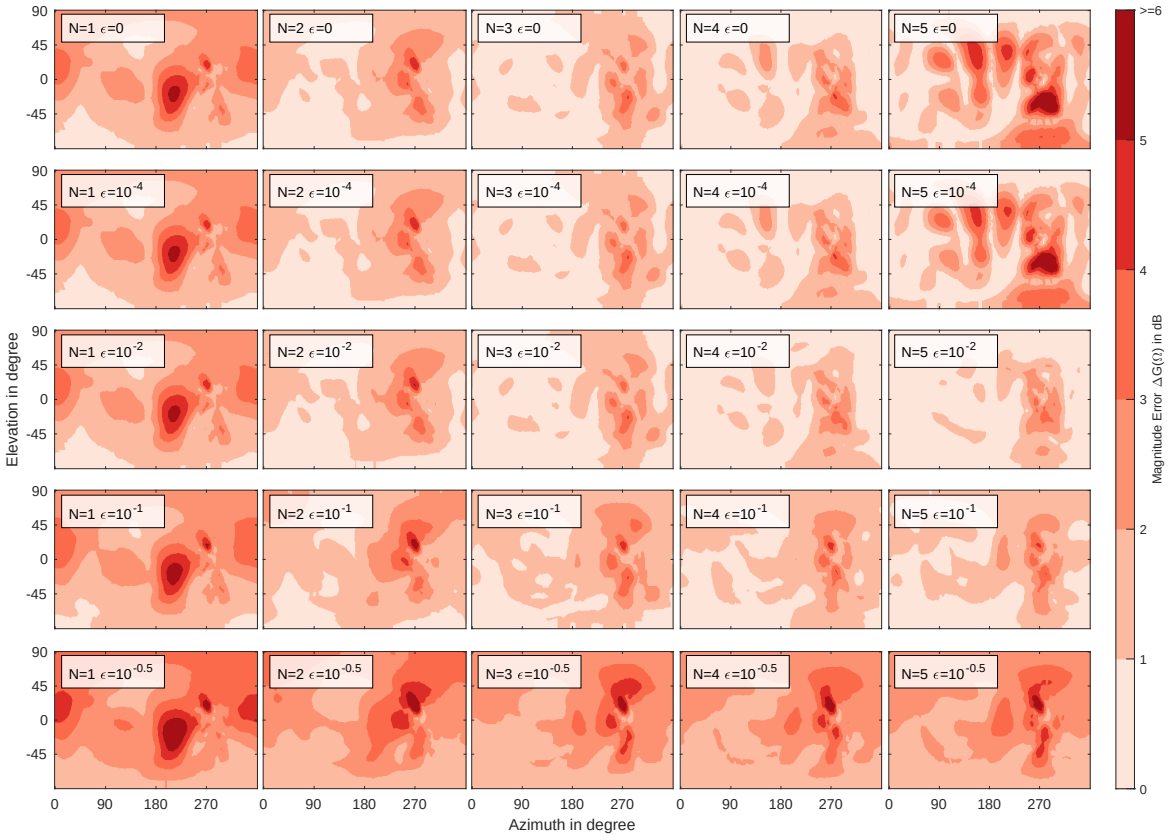

Figure S7. Left-ear magnitude error $\Delta G(\Omega)$ for grid *Irregular 2* at selected SH orders and regularization values ϵ. HRTF: Subject no. 10 from HUTUBS database.

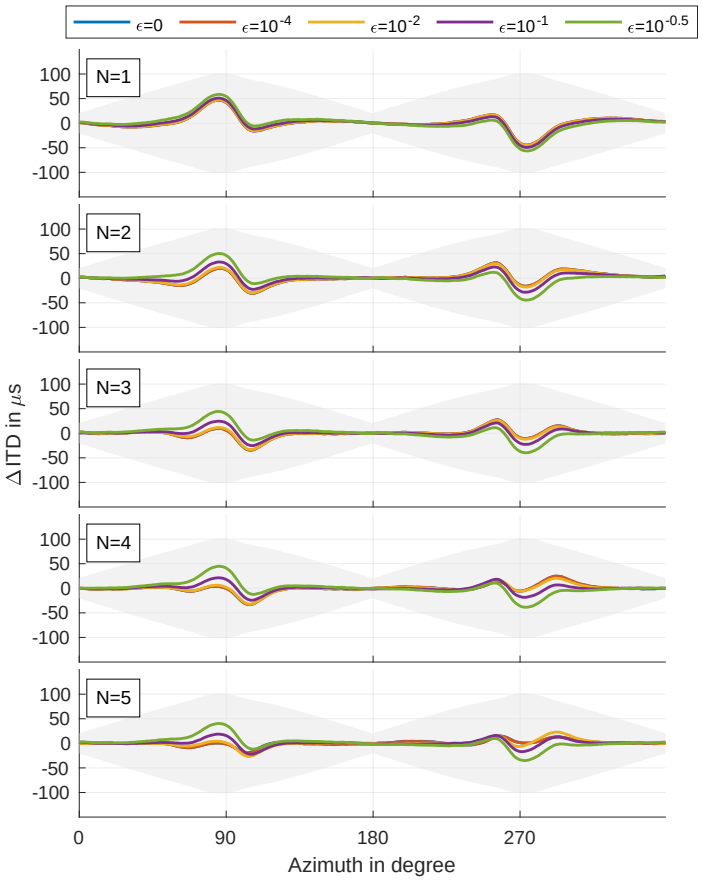

Figure S8. Difference in horizontal plane ITD relative to the dense reference for grid *Irregular 2* at selected SH orders and regularization values ϵ. The shaded area denotes the JND as a function of the reference ITD. HRTF: Subject no. 10 from HUTUBS database.

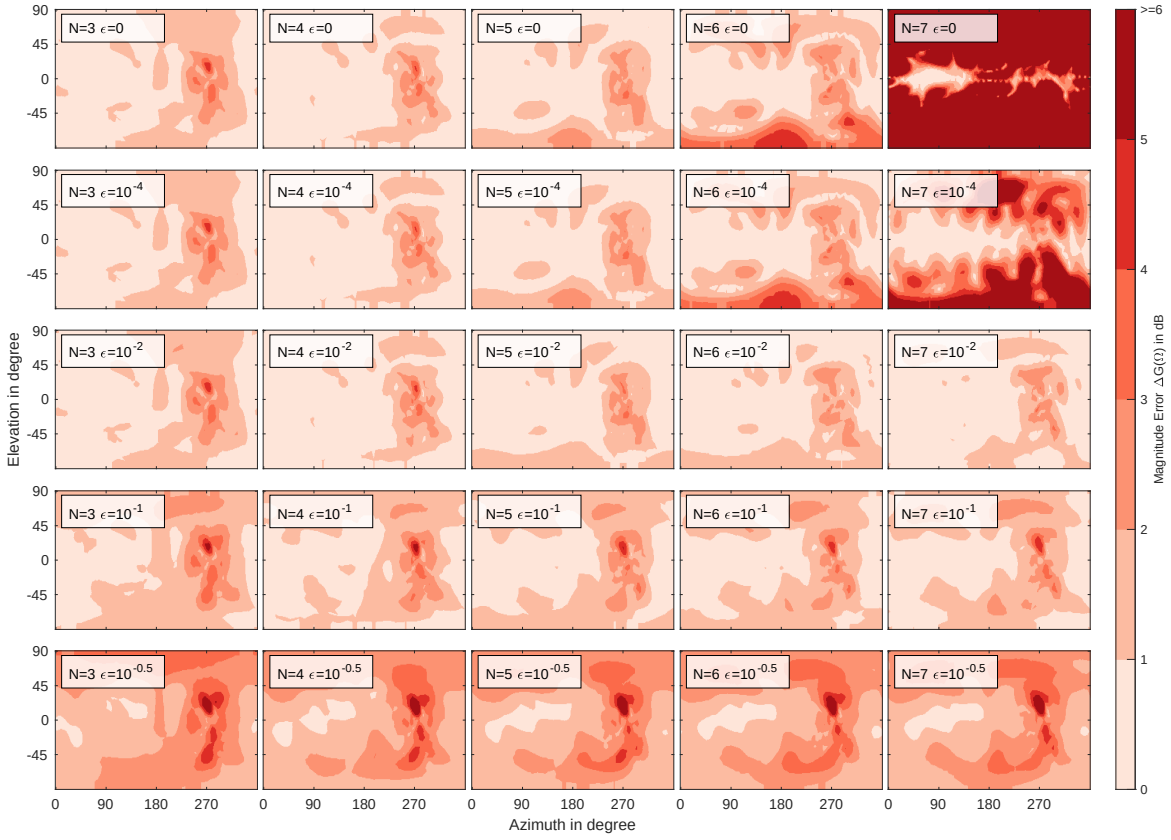

Figure S9. Left-ear magnitude error $\Delta G(\Omega)$ for grid *Irregular 3* at selected SH orders and regularization values ϵ. HRTF: Subject no. 10 from HUTUBS database.

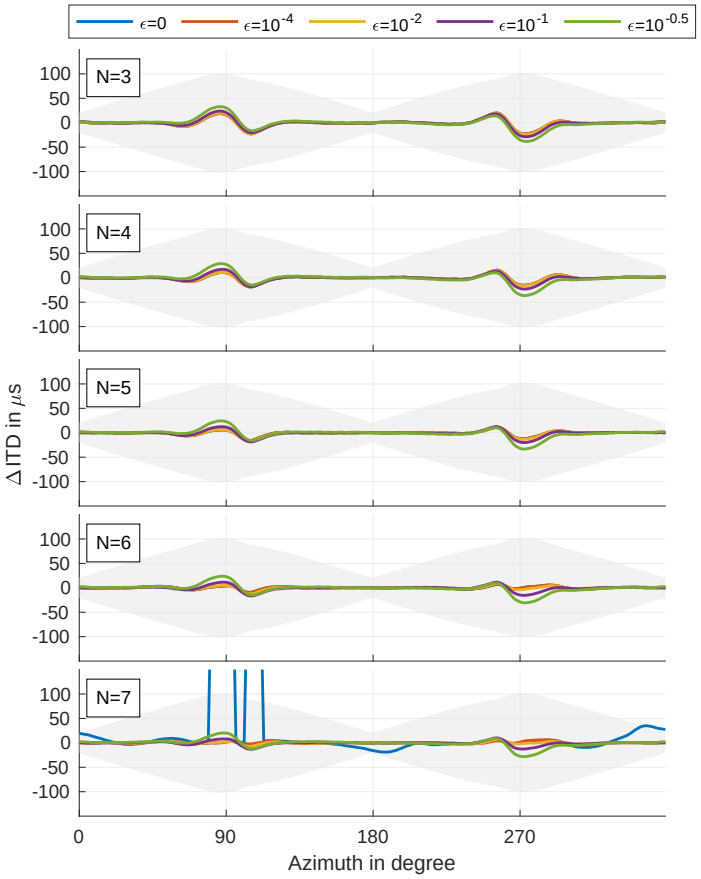

Figure S10. Difference in horizontal plane ITD relative to the dense reference for grid *Irregular 3* at selected SH orders and regularization values ϵ. The shaded area denotes the JND as a function of the reference ITD. HRTF: Subject no. 10 from HUTUBS database. The ITD difference for N=7 and $\epsilon = 0$ is partially too large for a reasonable display, thus it is clipped.

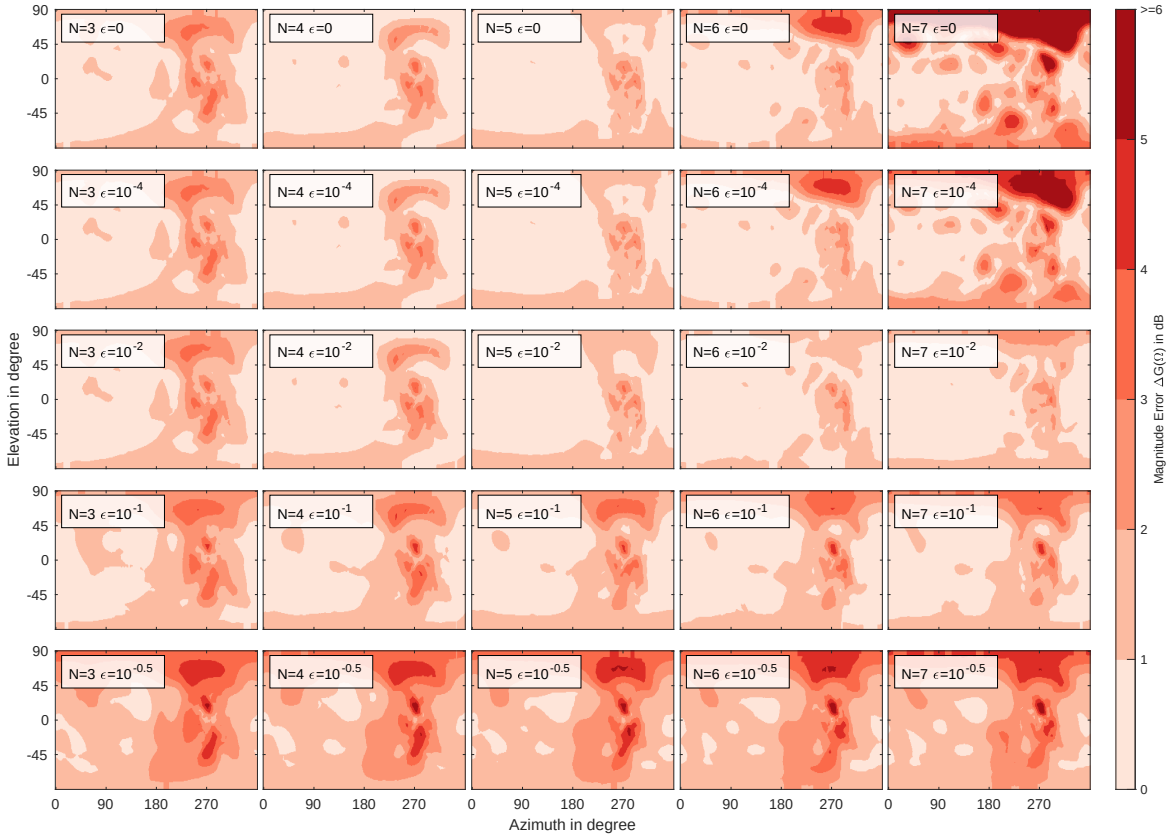

Figure S11. Left-ear magnitude error $\Delta G(\Omega)$ for grid *Irregular 4* at selected SH orders and regularization values ϵ. HRTF: Subject no. 10 from HUTUBS database.

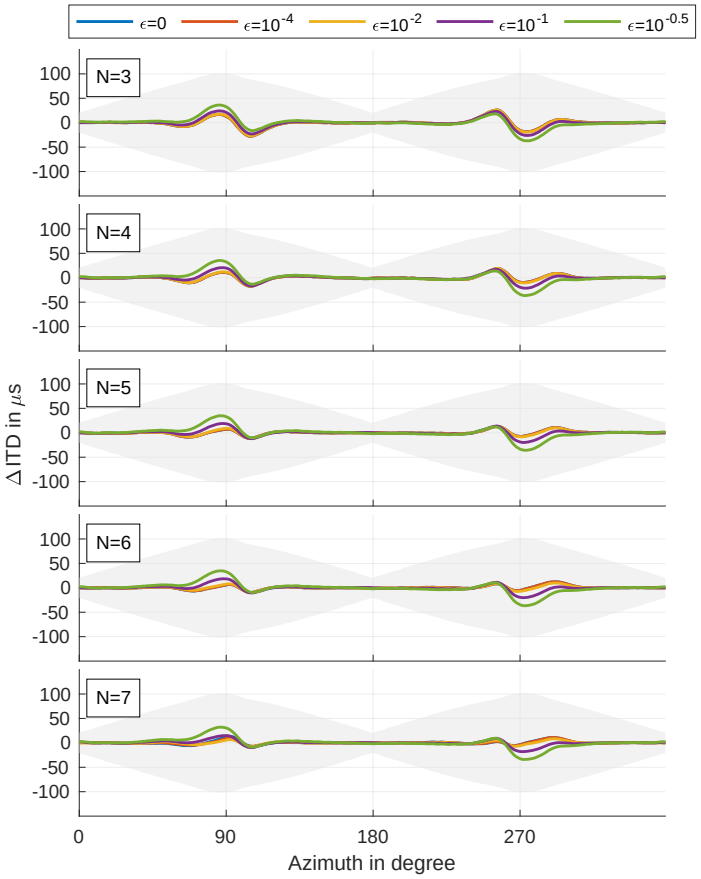

Figure S12. Difference in horizontal plane ITD relative to the dense reference for grid *Irregular 4* at selected SH orders and regularization values ϵ. The shaded area denotes the JND as a function of the reference ITD. HRTF: Subject no. 10 from HUTUBS database.

Figure S13. Left-ear magnitude error $\Delta G(\Omega)$ for grid *Irregular 5* at selected SH orders and regularization values ϵ. HRTF: Subject no. 10 from HUTUBS database.

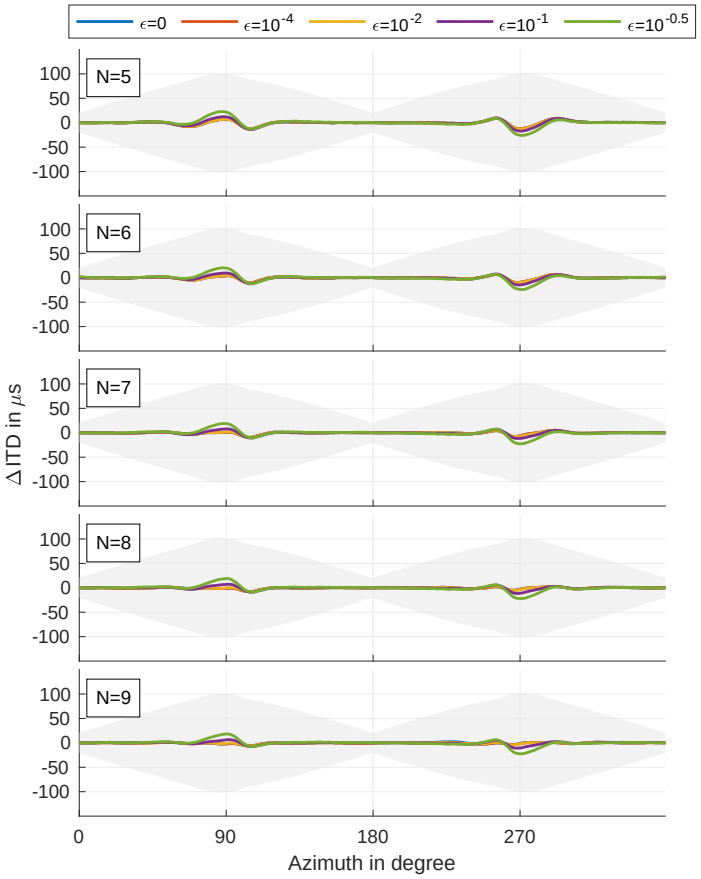

Figure S14. Difference in horizontal plane ITD relative to the dense reference for grid *Irregular 5* at selected SH orders and regularization values ϵ. The shaded area denotes the JND as a function of the reference ITD. HRTF: Subject no. 10 from HUTUBS database.

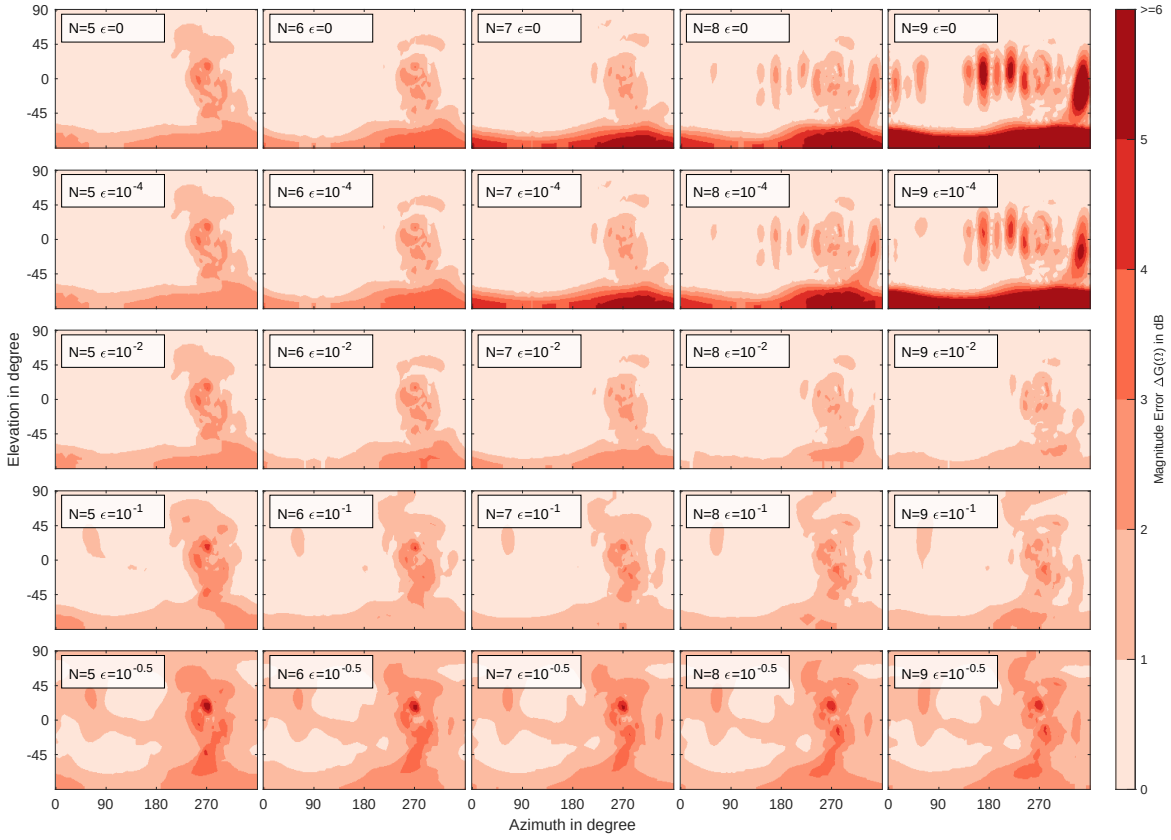

Figure S15. Left-ear magnitude error $\Delta G(\Omega)$ for grid *Irregular 6* at selected SH orders and regularization values ϵ. HRTF: Subject no. 10 from HUTUBS database.

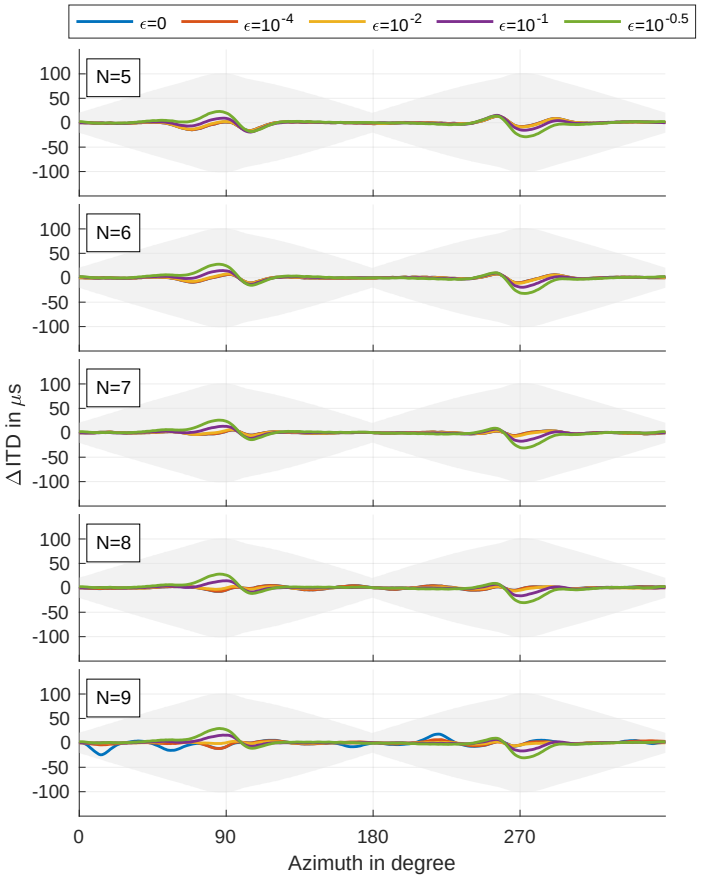

Figure S16. Difference in horizontal plane ITD relative to the dense reference for grid *Irregular 6* at selected SH orders and regularization values ϵ. The shaded area denotes the JND as a function of the reference ITD. HRTF: Subject no. 10 from HUTUBS database.

Figure S17. Left-ear magnitude error $\Delta G(\Omega)$ for grid *Gauss N=7* at selected SH orders and regularization values ϵ. HRTF: Subject no. 10 from HUTUBS database.

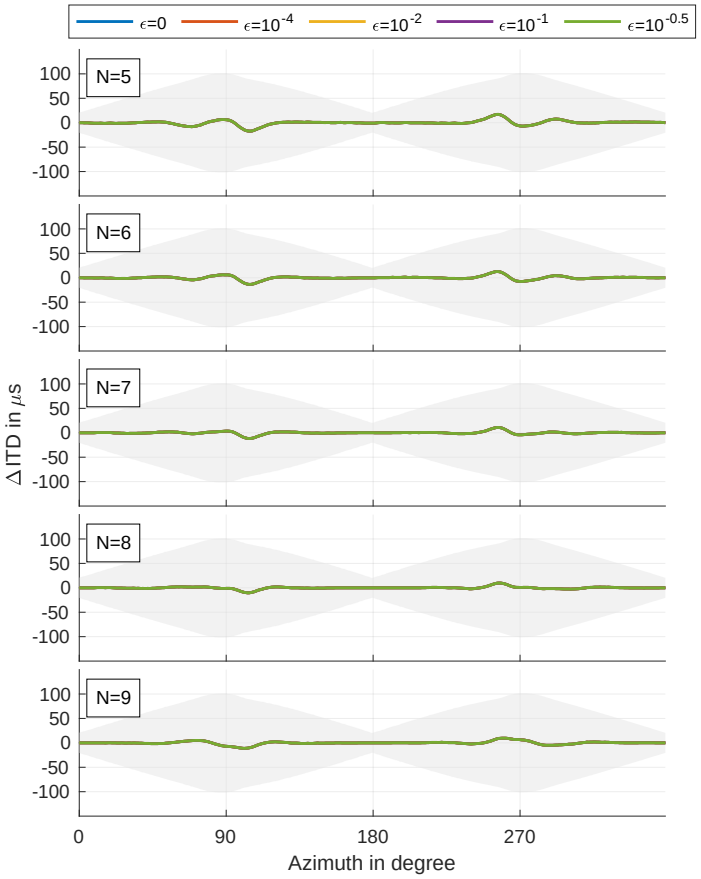

Figure S18. Difference in horizontal plane ITD relative to the dense reference for grid *Gauss N = 7* at selected SH orders and regularization values ϵ. The shaded area denotes the JND as a function of the reference ITD. HRTF: Subject no. 10 from HUTUBS database.

Figure S19. Left-ear magnitude error $\Delta G(\Omega)$ for grid *Lebedev N=7* at selected SH orders and regularization values ϵ. HRTF: Subject no. 10 from HUTUBS database.

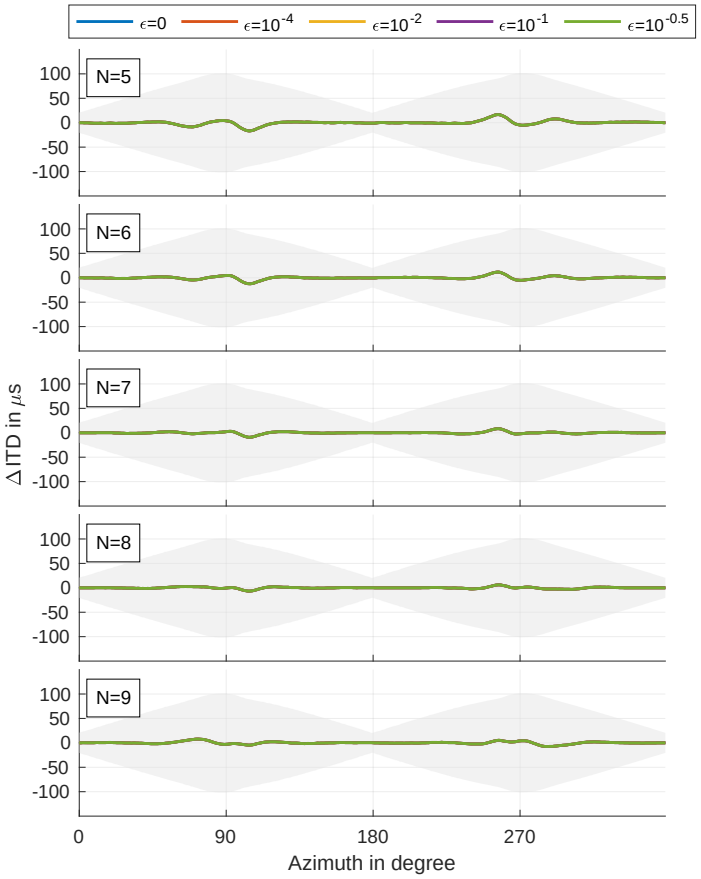

Figure S20. Difference in horizontal plane ITD relative to the dense reference for grid *Lebedev N = 7* at selected SH orders and regularization values ϵ. The shaded area denotes the JND as a function of the reference ITD. HRTF: Subject no. 10 from HUTUBS database.

REFERENCES

Ben-Hur, Z., Alon, D. L., Mehra, R., and Rafaely, B. (2019). Efficient Representation and Sparse Sampling of Head-Related Transfer Functions Using Phase-Correction Based on Ear Alignment. *IEEE/ACM Transactions on Audio Speech and Language Processing* 27, 2249–2262. doi:10.1109/TASLP.2019.2945479

Brinkmann, F. and Weinzierl, S. (2018). Comparison of head-related transfer functions pre-processing techniques for spherical harmonics decomposition. In *Proceedings of the AES International Conference on Audio for Virtual and Augmented Reality (AVAR)* (Redmond, WA, USA: AES), 311–320